molecular pharmaceutics

Article

Targeted delivery of a ligand-drug conjugate via formyl peptide receptor 1 through cholesterol-dependent endocytosis

Junlin Wang, Meiwan Chen, Shaoping Li, and Richard D Ye

Mol. Pharmaceutics, **Just Accepted Manuscript** • DOI: 10.1021/acs.molpharmaceut.9b00188 • Publication Date (Web): 08 May 2019

Just Accepted

ACS Publications

is published by the American Chemical Society. 1155 Sixteenth Street N.W., Washington, DC 20036

Targeted delivery of a ligand-drug conjugate via formyl peptide receptor 1 through cholesterol-dependent endocytosis

Junlin Wang[1], Meiwan Chen[1], Shaoping Li[1], Richard D. Ye[1]*

[1] Institute of Chinese Medical Sciences and State Key Laboratory of Quality Research in Chinese Medicine, University of Macau, Macau Special Administrative Region, China

*Send correspondence to: Richard D. Ye, University of Macau, Tel: +853 88224690, Fax: +853 28841358, E-mail: richardye@um.edu.mo

Abstract:

G protein-coupled receptors (GPCRs) undergo ligand-induced internalization that carries the cognate ligands into intracellular compartments. The present study explores this property for use of formyl peptide receptor 1 (FPR1), a class A GPCR that binds formylated peptides, as a potential target for drug delivery. A pH-sensitive peptide-drug conjugate consisting of doxorubicin (DOX), *N*-ε-maleimidocaproic acid hydrazide (EMCH) and the formyl peptide fMet-Leu-Phe-Cys (abbreviated as DEF) was prepared. DEF retained pharmacological activities of formyl peptides in binding to FPR1 and mobilization of Ca^{2+} from intracellular stores. However, the conjugated DOX was no longer cell membrane-permeable and relied on FPR1 for cellular entry. DOX was released from DEF into acidic compartments labeled with fluorescent trackers for endosomes. Treatment of cells with pharmacological inhibitors that block clathrin- or caveolae-mediated endocytosis did not abrogate FPR1-dependent DEF internalization, nor did inhibition of macropinocytosis and phagocytosis. In contrast, cholesterol depletion abrogated DEF internalization through FPR1, suggesting characteristics of cholesterol-dependent uptake mediated by a cell surface receptor. These results demonstrate the possibility of using FPR1 for targeted drug delivery.

Key words: G protein-coupled receptors, receptor internalization, targeted drug delivery, pH-sensitive peptides conjugates, formyl peptides.

Abbreviations

GPCRs, G protein-coupled receptors; FPR1, formyl peptide receptor 1; DOX, doxorubicin; MDC, monodansylcadaverine; CytoD, cytochalasin D; CytoB, cytochalasin B; MβCD, methyl-β-cyclodextrin; CHC, clathrin heavy chain; CAV1, caveolin-1; Pak1, p21-activated kinase 1.

1. Introduction

Small molecules enter into cells mainly through simple diffusion, passive diffusion (including channel-mediated diffusion and carrier-mediated diffusion) and active transport [1]. With simple diffusion, the substance passes through plasma membrane without the aid of energy and integral membrane proteins. The substance diffuses in a concentration gradient-dependent manner, *i.e.*, from a high concentration compartment to a low concentration compartment. Similarly, passive diffusion does not need energy and the moving direction of the substance is also from high concentration to low concentration. In contrast, active transport moves molecules against a concentration gradient. A carrier, usually an integral membrane protein, is required for active transport of molecules.

In comparison, macromolecules entry into cells is mainly mediated by cell surface receptors through different endocytic mechanisms, including clathrin-mediated endocytosis, clathrin-independent endocytosis (such as caveolae-mediated endocytosis), macropinocytosis and phagocytosis [2-5]. A well-documented example is the transferrin receptor (TfR), a dimeric carrier protein for transport of transferrin through clathrin-mediated endocytosis [6] . Another example is the low-density lipoprotein receptor (LDLR) that binds cholesterol apolipoproteins and mediates the transport of LDL into cells through clathrin-dependent endocytosis [7] . The insulin receptor (IR) binds insulin and carries it into cells through caveolae-mediated endocytosis [8]. In addition to these receptors, the folate receptor, CD44 receptor and sigma receptor are also involved in the transport of extracellular substances [9]. Clathrin-mediated endocytosis is characterized by the formation of clathrin-coated vesicles that consist of the clathin proteins (termed triskelion and contains three heavy chains and three light chains), adaptor protein-2 (AP2), dynamin and other associated proteins [2]. This pathway is most extensively studied among all known endocytic pathways. It has been reported that sucrose and monodansylcadaverine (MDC) can block this endocytosis pathway [10]. The best studied clathrin-independent endocytosis is the caveolae-mediated endocytosis. It is characterized by the formation of 60-80 nm flask-shaped caveolae vesicles. Caveolae has 3 isoforms, caveolin-1 (CAV1), caveolin-2 (CAV2) and caveolin-3 (CAV3) [11] that are sensitive to the inhibitor filipin[12] . Macropinocytosis is a non-selective endocytic process driven by the actin cytoskeleton. It is often used for engulfing

external fluid and soluble proteins through the formation of membrane ruffles via actin polymerization, which may be activated by Rac and Cdc42 via the p21-activated kinase 1 (Pak1) [13]. Pak1 activity also plays an important role in the closure of macropinocytic cups[14] . As an inhibitor of macropinocytosis, cytochalasin D (Cyto D) has been used in studies of this pathway [15]. Phagocytosis is also an actin-based endocytotic mechanism that is used for internalization of large particles such as dead cells and microbial pathogens such as bacteria. Phagocytosis occurs not only in specialized cells such as monocytes, macrophages and mast cells but also in non-professional phagocytes including epithelial cells, hepatocytes and endothelial cells [16-18]. Phagocytosis can be inhibited by cytochalasin B (Cyto B) [19].

The formyl peptide receptors (FPRs) are rhodopsin-like G protein-coupled receptors (GPCRs) that play an important role in host defense against bacterial infection [20]. In humans, there are three FPRs: FPR1, FPR2 and FPR3 [21]. FPR1 and FPR2 are expressed at high levels in both peripheral blood monocytes and neutrophils, but FPR2 has a lower affinity for the classic tripeptide fMet-Leu-Phe (fMLF) compared to FPR1. In addition, binding and activation of FPR2 rely heavily on the composition of the C-terminal amino acids, such as in the case of Trp-Lys-Tyr-Met-Val-D-met (WKYMVm) [22]. FPR3 is expressed only in monocytes and FL2 is one of the very few endogenous ligands for this receptor [23]. It has been reported that FPR1 binds a ligand, such as fMLF, and carries the ligand into cells [24-25]. This property makes FPR1 a potential target for drug delivery, in addition to mediating bactericidal activities. Among the peptide ligands of FPR1, *N*-formylated peptides such as fMLF have been extensively studied. fMLF is an *E.coli*-derived tripeptide and the smallest formyl peptide with full agonistic activities [26]. The formyl peptides with five and six amino acid residues that are conjugated to the fluorescent dye FITC (fMLFFK-FITC and fMLFFFK-FITC) can still bind to FPR1 despite a bulky FITC molecule attached to its C-terminus [27]. This observation shows that FPR1 binding is less sensitive to the length and C-terminal composition of formyl peptides [22]. It is therefore predicted that modification of the FPR1 ligands is feasible without losing their affinity for the receptor. In the present study, the possibility of using FPR1 as a target for drug delivery was explored using transfected cells expressing the receptor. Formyl peptides were synthesized using the core sequence of fMLF with C-terminal amino acid

extensions and substitutions, resulting in peptides that may be coupled through a linker to a drug molecule. The modified ligands were tested for retention of FPR1-activating properties in calcium mobilization assays and binding assays. One of the peptides (fMLFC) was chosen for coupling to doxorubicin (DOX) as a drug conjugate. DOX is an anti-cancer drug that enters into cells easily through permeabilization and goes to the nucleus for its function. The DOX conjugate, predicted to have lost its cell membrane permeability in complex with fMLF, was then used as a probe for testing of targeted delivery through FPR1. Our results show that the DOX conjugate was excluded from diffusion through plasma membrane, and was found in the endosomes in a process that was dependent on FPR1. These findings suggest the feasibility of using FPR1 for targeted delivery of drugs that are otherwise cell permeable.

2. Materials and methods

2.1. Materials

Unconjugated formylated peptides were synthesized at GL Biochem, Shanghai, China. *N*-formyl-Met-Leu-Phe-Ile-Ile-Lys-fluorescein isothiocyanate (fMLFIIK-FITC) was synthesized by SynPeptide Shanghai, China. The siRNA used in this study was purchased from RiboBio, Guangzhou, China. Doxorubicin hydrochloride was purchased from Beijing Huafeng United Technology, China. fMLF, cytochalasin D (CytoD), sucrose, filipin III, monodansylcadaverine (MDC), lovastatin , methyl-β-cyclodextrin(MβCD), nocodazole, *N*-ε-maleimidocaproic acid hydrazide, horseradish peroxidase (HRP), trifluoroacetic acid salt (EMCH) and trifluoroacetic acid (TFA) were obtained from Sigma-Aldrich, St. Louis, MO, The ProLong™ Diamond antifade mountant and TRIzol® Reagent were purchased from Thermo Fisher Scientific, Waltham, MA. Early endosome-RFP and lysotracker yellow HCK-123 were purchased from Molecular Probes, Eugene, OR. Alexa Fluor® 647-labeled mouse anti-human fMLP receptor (Clone 5F1, RUO) was purchased from BD Biosciences, San Jose, CA. The FLIPR calcium 5 reagent was obtained from Molecular Devices, Sunnyvale, CA. Lipofectamine™ 3000 transfection reagent was purchased from Invitrogen, Carlsbad, CA.

2.2. Cell culture

HeLa cells (ATCC CCL2) were cultured in DMEM containing 10% fetal bovine serum

(FBS), 100 U/mL penicillin and 100 μg/mL streptomycin. Stable cell line of rat basophilic leukemia cell line RBL-2H3 (ATCC CRL 2256) expressing FPR1 (RBL-FPR1 [28]) was maintained in DMEM supplemented with 20% FBS and 250 μg/mL G418. All cells were cultured under standard incubation conditions (5% CO_2, 37°C).

2.3. Calcium mobilization

FPR1 stable transfectants (RBL-FPR1 cells) were grown to 95% confluence in 96-well plates with black wall and clear round bottom. The cells were incubated with the FLIPR Calcium 5 reagent for 1 h at 37°C according to the manufacturer's protocol. Different concentrations of peptides or the DOX conjugate (DEF) were added to the 96-well plates before measurement on a FlexStation III (Molecular Devices). The samples were excited at 485 nm. The data were read at an emission wavelength of 525 nm and acquired using the SoftMax Pro 6 software (Molecular Devices).

2.4. Ligand binding

RBL-FPR1 cells were harvested and resuspended to $1x10^5$/mL in HBSS buffer (contain 0.5% BSA and 20 mM HEPES) on ice. For saturation binding, different concentrations of fMLFIIK-FITC were used. Nonspecific binding and total binding were detected in the presence and absence of unlabeled peptide (fMLFIIK, 50 μM). The cells were then incubated for 1 h on ice and median fluorescent intensity (MFI) of FITC fluorescence was measured on a flow cytometer. Maximal binding sites on the cell membrane were estimated with Molecules of Equivalent Soluble Fluorochrome (MESF) of the FITC-conjugated standard beads (Polysciences, Warrington, PA). For competition binding, different concentrations of unlabeled peptides or synthesized compounds were added with 125 nM of fMLFIIK-FITC. The cells were incubated for 1 h on ice and MFI of FITC was measured by flow cytometry (BD Accuri™ C6).

2.5. Synthesis and characterization of DEF

2.5.1. Synthesis of DEF

DOX (5.2 mg) and EMCH (9.2 mg) were mixed in 1.75 mL of methanol. Then 0.5 μL trifluoroacetic acid was added and the solution was stirred at room temperature for 48 h in the dark [29]. The reaction solution was concentrated with N_2 blow to a volume of 500 μL. Five

mL ethyl acetate was added into the reaction solution to precipitate the product DOX-EMCH (DE). The red solid DE was isolated by centrifugation at 1500 x *g* for 1 min before addition of another 5 mL of ethyl acetate for washing and then centrifugation at 1500 x *g* for 1 min. The products were dried with N_2 blow. The dried DE and 9.2 mg of fMLFC was dissolved in 2.0 mL DMF and reacted for 24 h at room temperature with gentle agitation. The target product (DEF) was purified by preparative HPLC. The purity of DE and DEF was determined by HPLC.

2.5.2. High performance liquid chromatography (HPLC)

The purity of DE and DEF were detected by HPLC (Waters e2695, Waters Corporation, Milford, MA) equipped with a UV-visible detector (wavelength at 254 nm). The analysis was performed on a reverse phase C18 column (4.6 x 250 mm, 5 μm particle size, Agilent Technologies). The mobile phase consisted of solvent A (27.5% acetonitrile mixed with 72.5% 20 mM, pH 7.0 in PBS buffer) and solvent B (acetonitrile). Gradient elution method with a flow rate of 1 mL/min was applied in the following manner: 100%A (0 min) →100%A (15 min) →41.4%A (20 min) →41.4%A (25 min) →100%A (30 min).

2.5.3. Preparative HPLC

The crude reaction solution of DEF was purified by preparative HPLC (Shimadzu LC20AP, Shimadzu Corporation, Kyoto, Japan) equipped with a UV-visible detector and a C18 preparative column (9.4 × 250 mm, 5 μm, Zorbax Agilent). The mobile phase consisted of solvent A (acetonitrile) and solvent B (Milli Q water). Gradient elution method with a flow rate of 2 mL/min was applied in the following manner: 27.5%A (0 min) →27.5%A (20 min) →70%A (25 min) →70%A (35 min) →90%A (36 min) →90%A (45 min). Fractions were collected and dried at 42°C in a vacuum drying oven.

2.5.4. Mass spectrometry

Mass spectra of DEF was detected by Thermo LTQ Orbitrap XL (Thermo Fisher Scientific, Waltham, MA) equipped with an electrospray ion source. The analysis was performed on the positive ion mode. The spectra of the samples were acquired under the following condition: m/z range 150–2000 Da, spray voltage 4.5KV, capillary voltage 35V, capillary temperature 275°C. Nitrogen was used as a sheath gas (flow rate: 5 arb). Samples were dissolved in methanol for analyses.

2.6. Cellular uptake

To study the cellular uptake behavior of DOX, DE, DEF, and mixtures of DOX, EMCH, fMLFC (D,E,F mixture), HeLa cells and HeLa cells transiently transfected with FPR1-GFP (HeLa FPR1-GFP) were plated on a glass coverslip in a 24-well plate. Cells were treated with DOX (5 μM), DE (equivalent DOX concentration: 5 μM), DEF (equivalent DOX concentration: 5 μM) and D,E,F mixture (DOX, EMCH and fMLFC concentration: 5 μM). Then cells were washed by PBS and fixed with 4% paraformaldehyde (PFA) for 10 min at room temperature. The coverslips were mounted on glass slides with Diamond antifade mountant (Thermo Fisher Scientific) and visualized by confocal microscopy (LEICA TCS SP8). Confocal images were taken with a 40× oil objective. The excitation wavelength of FPR1-GFP was set at 488 nm, the emission wavelength was collected at 493 to 525 nm. The excitation wavelength for DOX is 488 nm, the emission wavelength was collected at 625 to 750 nm. Colocalization of the tagged FPR1 with different compounds was analyzed by Pearson's correlation coefficient (Rr). Rr was widely used in quantification of colocalization level of two fluorescence channels. Rr values have a range of +1 (perfect correlation) to -1 (perfect anti-correlation), and 0 means no correlation [30].

2.7. FPR1 intracellular trafficking

To track the intracellular route of FPR1, early endosome and lysosome were stained with early endosome-RFP and lysotracker yellow HCK-123. HeLa cells transfected with FPR1-GFP or FPR1-mRuby2 were seeded on a glass coverslip in a 24-well plate and incubated for 18-24 h at 37°C. For endosome staining, 80 μL of endosome-RFP was added into 24-well plates and incubated at 37°C for 16 h for expression of the protein label. For lysosome stain, 10 μL lysotracker yellow HCK-123 was added into a 24-well plate, diluted to 2 μM, and incubated at 37°C for 1 h. Then the cells were treated with 5 μM fMLF (ligand of FPR1) at 37°C for 1 h to induce internalization of FPR1. The cells were washed with PBS and fixed with 4% PFA for 10 min at room temperature. The cells were finally stained for nuclei with 2 μg/mL Hoechst for 10 min at room temperature. The coverslips were mounted on glass slide with Diamond antifade mountant and visualized by confocal microscopy (LEICA TCS SP8). Confocal images were taken with a 40× oil objective. For Hoechst the excitation wavelength

was 405 nm, the emission wavelength was collected at 410 to 490 nm. For lysotracker the excitation wavelength was 488 nm, the emission wavelength was set between 493 and 525 nm. For endosome-RFP the excitation wavelength was 552 nm, the emission wavelength was from 569 to 700 nm.

2.8. Intracellular pH-induced release of DOX

To study the pH-induced release behavior of DEF, HeLa FPR1-GFP cells were plated on glass coverslip in a 24-well plate. Cells were treated with DEF (equivalent DOX concentration: 5 μM) for 1 h and 6 h at 37°C. Then the cells were washed with PBS at indicated time points, fixed with 4% PFA for 10 min at room temperature, and stained with 2 μg/mL Hoechst for 10 min at room temperature. The coverslips were mounted on glass slides with Diamond antifade mountant and visualized by confocal microscopy (LEICA TCS SP8). Confocal images were taken with a 40× oil objective.

2.9. Transfection with plasmid and siRNA

HeLa cells were transfected with FPR1-GFP or FPR1-mRuby2 using Lipofectamine 3000 (Invitrogen) according to the reagent protocol when cells were grown to 70% confluency. Then cells were incubated at 37°C with 5% CO_2 for 24 h - 48 h. For transfection of different kinds of siRNA [31-32] (**see Table 1**), the FPR1-GFP transfected HeLa cells (HeLa FPR1-GFP) were grown to 50% confluency and then transfected with Lipofectamine 3000 using the transfection protocol as described for DNA but did not add the P3000 reagent when diluting the siRNA. The final concentration of siRNA in the cell culture medium was 50 nM. The cells were incubated at 37°C with 5% CO_2 for 48 h before performing uptake experiment.

Table 1. siRNA sequence used in this study

siRNA target	Sequence
CHC	UAAUCCAAUUCGAAGACCAAUdTdT
CAV1	AGACGAGCUGAGCGAGAAGdTdT
PAK1	AUAACGGCCUAGACAUUCAdTdT

2.10. Q-PCR analysis

The siRNA-treated HeLa FPR1-GFP cells were lysed by the TRIzol® Reagent and total

RNA was isolated. cDNA was prepared by using a 5X PrimeScript RT Master Mix (Takara Bio, Otsu, Shiga, Japan). The cDNA was used along with SYBR premix Ex taq II (TAKARA BIO INC) according to the manufacture's protocal, then the reaction was perform on the ViiA 7 Real-Time PCR System. β-Actin served as an endogenous control.The Ct values were detected and normalized with an β-Actin. The mRNA Level was estimated by the 2-ΔΔCt method [33]. Cycle conditions were 95°C for 30 sec, followed by 40 cycles at 95°C for 5 sec and then 60°C for 60 sec. Sequence-specific primers are listed in **Table 2**.

Table 2. Primer sequence used for Q-PCR

Gene name	Forward primer 5′-3′	Reverse primer 5′-3′
CHC	TGATCGCCATTCTAGCCTTGC	CTCCCACCACACGATTTTGCT
CAV1	CATCCCGATGGCACTCATCTG	TGCACTGAATCTCAATCAGGAAG
PAK1	CAACTCGGGACGTGGCTAC	CAGTATTCCGGGTCAAAGCAT
β-Actin	AGAGCTACGAGCTGCCTGAC	AGCACTGTGTTGGCGTACAG

2.11. Pharmacological inhibition of endocytosis

For pharmacological inhibition studies, HeLa FPR1-GFP cells were seeded on glass coverslips in 24-well plates and grown for 18-24 h. The cells were subsequently pretreated with different endocytosis inhibitors at 37°C for 30 min in DMEM containing 0.5M sucrose, 100 μM monodansylcadaverine MDC, 5 μg/mL Filipin complex, 10 μM CytoD or for 2 h at 37°C in DMEM containing 10 μg/mL CytoB or for 2 h at 37°C in DMEM containing 10 μg/mL cytochalasin B (CytoB). Cells on the glass coverslips were washed 2 times with PBS, treated with 5 μM DEF at 37°C for 1 h, and then rinsed with PBS before fixing with 4% PFA for 10 min at room temperature. Finally, the cell nuclei were stained with 2 μg/mL Hoechst for 10 min at room temperature. The coverslips were mounted on glass slides with Diamond antifade mountant and visualized by confocal microscopy (LEICA TCS SP8, Leica Microsystems, Wetzlar, Germany). Confocal images were taken with a 40× oil objective.

2.12. Plasma membrane cholesterol depletion

HeLa FPR1-GFP cells were seeded on glass coverslips in 24-well plates for 18-24 h. The

cells were treated with 10 mM MβCD in the presence of 3 μg/mL Lovastatin at 37℃ for 1 h in DMEM [15]. Cells on the glass coverslips were washed 2 times with PBS and then treated with 5 μM DEF at 37℃ for 1 h, then rinsed with PBS and fixed with 4% PFA for 10 min at room temperature. The cells were finally stained with 2 μg/mL Hoechst for 10 min at room temperature. The coverslips were mounted on glass slide with diamond antifade mountant and visualized by confocal microscopy (LEICA TCS SP8). Confocal images were taken with a 40× oil objective.

2.13. Microtubule disruption

HeLa FPR1-GFP cells were seeded on glass coverslips in 24-well plates and grown for 18-24 h. The cells were treated with 10 μg/mL nocodazole (Sigma) at 37°C for 1 h in DMEM [15, 34]. The cells on the glass coverslips were washed 2 times with PBS and treat with 5 μM DEF at 37°C for 1 h, then rinsed with PBS and fixed with 4% PFA for 10 min at room temperature. The cells were finally stained with 2 μg/mL Hoechst for 10 min at room temperature. The coverslips were mounted on glass slides with Diamond antifade mountant and visualized by confocal microscopy (LEICA TCS SP8). Confocal images were taken with a 40× oil objective.

2.14. Cell surface receptor detection

HeLa FPR1-GFP cells were harvested, washed with PBS and resuspended in DMEM. The cells were subsequently pretreated with different pharmacological inhibitors at 37°C for 30 min in DMEM containing 10 μM Cyto D, 5 μg/mL Filipin complex, 100 μM MDC, 0.5 M sucrose, or for 2 h at 37°C in DMEM containing 10 μg/mL Cyto B or for 1 h at 37°C in DMEM containing 10 mM MβCD / 3 μg/mL Lovastatin, 10 μg/mL nocodazole for 1h, followed by incubation with 5 μM DEF. The cells in sample tubes were placed on ice and washed 3 times with ice-cold PBS and blocked with 5% BSA for 1 h on ice. The cells were then stained with anti-FPR1 antibody on ice for 30 min and washed with ice-cold PBS twice. The cell surface receptors were quantified by flow cytometry (BD Accuri™ C6). GFP-positive cells were gated in FL1 channel and analyzed for cell surface receptor number with the anti-FPR1 antibody in FL4 channel.

2.15. MTT Assay

The cytotoxicity of different pharmacological inhibitors was detected using MTT assay. HeLa cells were plated on the 96-well plate and cultured for 24h at 37°C. Then the compounds (0.5 M sucrose, 100 μM MDC, 5 μg/mL Filipin complex, 10 μM Cyto D, 10 μg/mL Cyto B, 10 mM MβCD / 3 μg/mL Lovastatin, 10 μg/mL nocodazole) were added to the wells and incubated for 2h at 37°C. After an addition of 10 μL MTT (5 mg/mL) to each well, the cells were incubated for 3 h at 37°C until purple precipitate was visible. Then 100 μL DMSO was added to dissolve the precipitate and the absorbance of the sample were detected in a microplate reader (SpectraMax® M5, Molecular Devices) at 570 nm.

3. Results

3.1. Functional characterization of different formyl peptides

3.1.1. Comparison of different formyl peptides in Ca^{2+} flux assays

A number of peptides with *N*-formyl group and modified C-terminal residues were synthesized (Fig. 1A). To allow reaction with the maleimide group in the linker, these peptides contained a cysteine (Cys, C) in their carboxyl termini. It is well known that formyl peptides of different compositions may have different abilities to induce functional response[26]. The pharmacological properties may also change after conjugation of the peptides to DE. As a result, these peptides (fMLF, fMLFC, fMLFKC, fMLFGGC and fMLFGGKC, Fig. 1A) were first examined in functional assays before conjugating to DE. Ca^{2+} flux was an early response mediated by FPR1 upon agonist binding. The representative calcium traces and dose-dependent curves were shown in Fig. 1B and 1C. All peptides induced Ca^{2+} influx. Among these peptides, fMLFC had the highest potency at FPR1 (EC_{50} = 3.02 x 10^{-8} M). In comparison, the two peptides ending with –KC performed poorly in Ca^{2+} flux assays at concentration of 10^{-7} M.

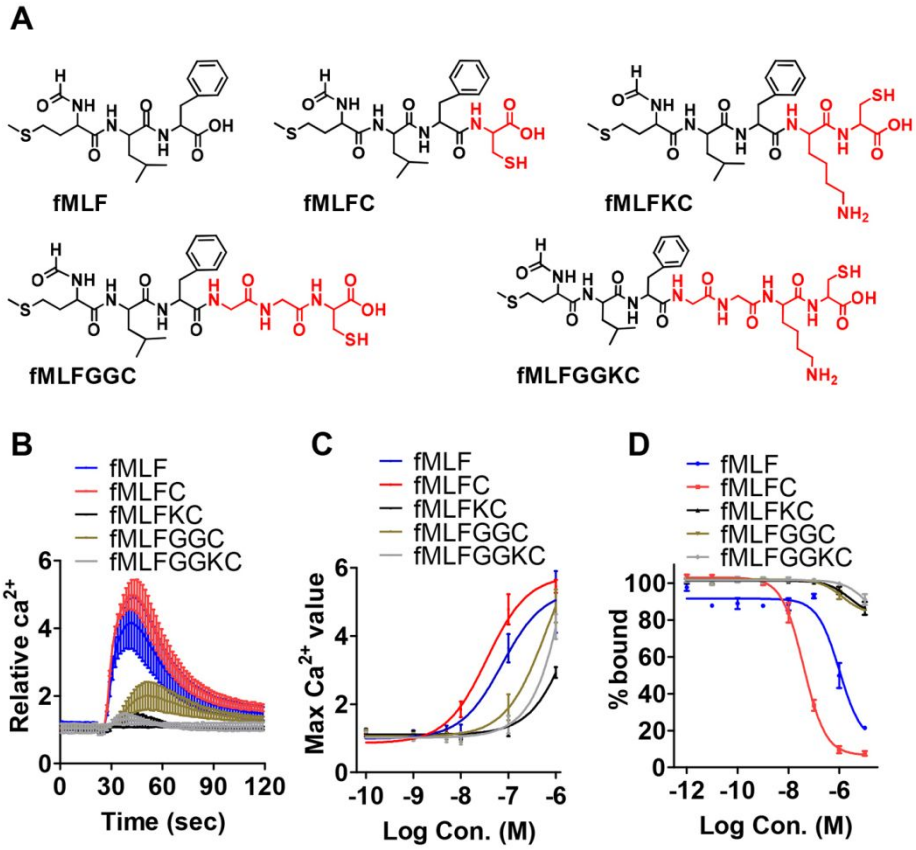

Fig. 1. Effects of different formyl peptides on calcium mobilization in RBL-FPR1 cell. (A) The structures of the formyl peptides fMLF, fMLFC, fMLFKC, fMLFGGC and fMLFGGKC. (B) Real-time measurement of Ca^{2+} influx in response to the peptides at a concentration of 10^{-7} M. Relative Ca^{2+} values are shown as the ratio of the reading over basal level in unstimulated cells. (C) Dose curves of Ca^{2+} mobilization base on peak values. The data are expressed as means ± SEM from 3 experiments. (D) Competition binding of different peptides against fMLFIIK-FITC (125 nM). The data are expressed as means ± SEM from 3 experiments.

The binding behavior of the peptides was next examined. A FITC-labeled formyl peptide (fMLFIIK-FITC) [35] was synthesized for binding assays using flow cytometry. Non-specific binding was relatively low, and the dissociation constant (K_d) was determined to be 3.4 nM after calibration of fluorescence intensity with standard fluorescence sphere (data not shown). Competitive binding assay was carried out with different peptides. As shown in Fig. 1D, fMLFC effectively competed with fMLFIIK-FITC for binding to FPR1 with an IC_{50} of 3.95 x 10^{-8} M. In comparison, fMLFKC, fMLFGGC and fMLFGGKC could not effectively compete off fMLFIIK-FITC binding. Based on the results from binding and calcium flux assays, fMLFC

was chosen for synthesis of DEF.

3.2. Preparation and characterization of DEF

DEF was synthesized according to the procedures described in Fig. 2. The intermediate product (DE) was used to conjugate the peptide and polymer through the Michael addition reaction [36-40]. HPLC was used to monitor the purity after each synthesis step. As shown in Fig. 3A, the retention time (RT) of DOX was 10 min. After reacting with EMCH, most DOX became DE (Fig. 3B). After reacting DE with fMLFC, the RT of DEF (20 min) was shifted by 1 min compared with DE (19 min, Fig. 3B and 3C). The purity of DEF was approximately 90% after purification by preparative HPLC (Fig. 3D). The mass spectrometry result provided further evidence that DE (m/z 751.29) and DEF (m/z 1291.51) were synthesized successfully (Fig. 3E, 3F). This acid-sensitive peptide conjugate was expected to release DOX in the acid compartments, such as lysosomes and endosomes, through the cleavage of a hydrazine bond between DOX and EMCH [41]. It was found that the solubility of DEF was poor. The possible reason for the reduction in solubility was that the functional group (fMLFC) contained a hydrophobic amino acid, making the product (DEF) less soluble in water.

Ca^{2+} flux was readily induced by DEF (Fig. 3G and 3H). The potency at FPR1 was similar between DEF (EC_{50} = 8.72 x 10^{-8} M) and fMLF (EC_{50} = 7.50 x 10^{-8} M). It indicated that the ability to induce Ca^{2+} flux was well preserved in DEF. As expected, the intermediate product (DE) could not induce intracellular Ca^{2+} flux at different concentrations due to the absence of a formyl peptide in the complex. Therefore, fMLFC modification through complex formation did not change its functional properties in activating FPR1. DE and DEF were also used in the competition assay to estimate its affinity for FPR1 (Fig. 3I). The results demonstrated a high affinity of DEF for FPR1 (IC_{50} = 4.82 x 10^{-7} M, Fig. 3I). In comparison, DE did not compete for FPR1 binding. The affinity of DEF was slightly lower than that of fMLFC due to coupling to DE, but the ability to binding to FPR1 was retained.

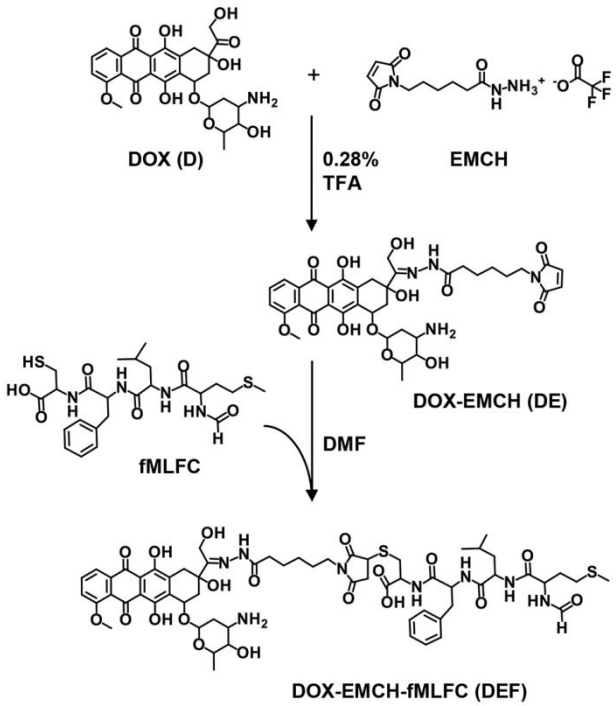

Fig. 2. The synthesis of DOX-EMCH-fMLFC (DEF)

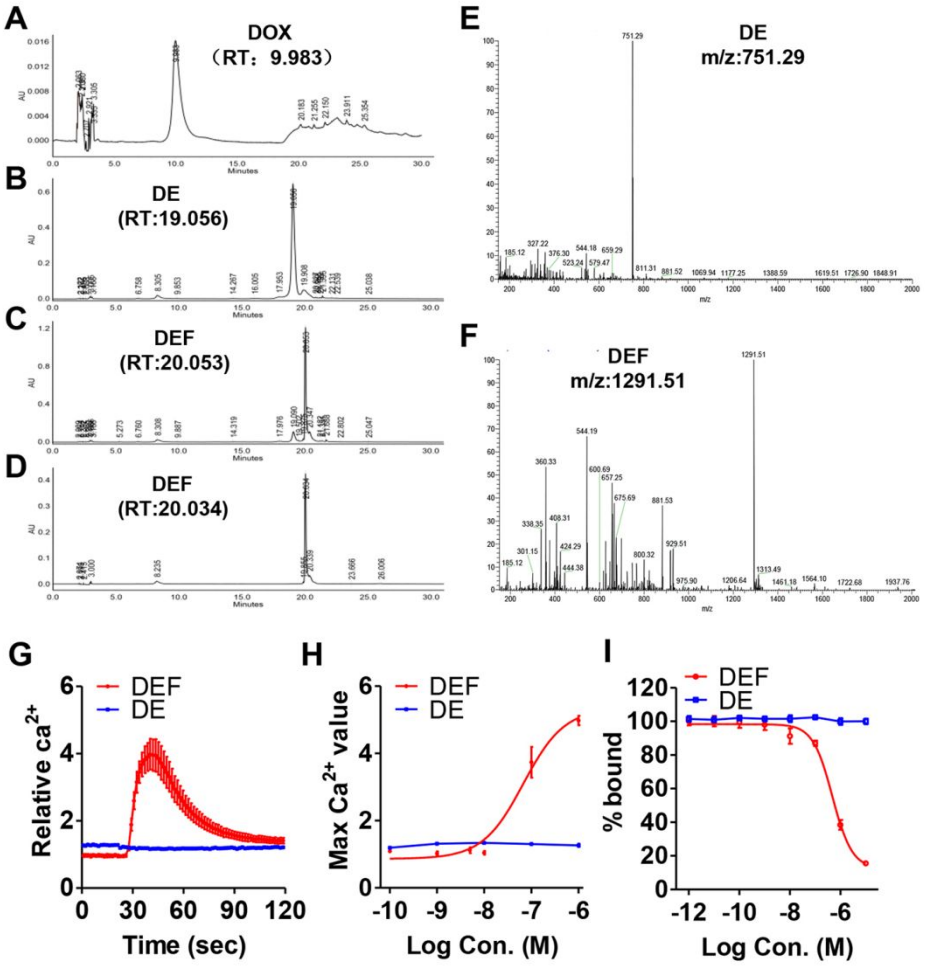

Fig. 3. Characterization of DEF. (A) HPLC chromatograms of DOX. RT: retention time. (B) HPLC chromatograms of DOX and EMCH reaction products that were purified by ethyl acetate precipitation. (C) HPLC chromatograms of DE and fMLFC reaction products. (D) HPLC chromatograms of DEF purified by preparative HPLC. (E) and (F), mass spectra of DE and DEF, respectively. (G) Relative Ca^{2+} influx in response to DE and DEF at a concentration of 1 x 10^{-7} M. Relative Ca^{2+} flux is shown as the ratio of the reading over base line. (H) Dose-dependent curves based on peak values of Ca^{2+} mobilization. (I) Competition binding of DE and DEF against fMLFIIK-FITC (125 nM). All data are expressed as means ± SEM from 3 experiments.

3.3. Cellular uptake of DOX, DE, DEF and the mixture of D, E and F

In order to test whether DEF could enter into cells through FPR1 internalization, uptake assays were carried out using cell lines expressing a GPF-tagged FPR1 (FPR1-GFP). The tagged FPR1 allowed determination of its colocalization with different compounds using Pearson's correlation coefficient (Rr). Rr was widely used in quantification of colocalization levels based on two fluorescence channels. The compounds tested were DOX, DE, DEF and a mixture of DOX, EMCH and fMLFC (D, E, F mixture). In control cells without FPR1-GFP expression, both the green channel (FPR1-GFP) and the red channel (DEF) were blank (Fig. 4A), suggesting that DEF could not permeate through plasma membrane. DEF entered into the HeLa FPR1-GFP cells through internalization, with visible cytoplasmic distribution of the green fluorescence (Fig. 4B). The intensity of red fluorescence was much higher in HeLa FPR1-GFP than in HeLa cells when incubated with DEF (Fig. 4D). The Rr value (0.5) demonstrated that the internalized DEF was colocalized with FPR1-GFP (Fig. 4C). These results demonstrated that DEF entered into HeLa FPR1-GFP cells in a FPR1-dependent manner. In DOX- and D, E, F mixture-treated HeLa and HeLa FPR1-GFP cells, red fluorescence was detected, suggesting that unconjugated DOX entered into cells without FPR1. In HeLa FPR1-GFP cells, the green fluorescence remained on cell surface (Fig. 4B), suggesting that the entry of DOX did not induce internalization of FPR1-GFP. However, incubation with the D, E, F mixture induced FPR1-GFP internalization due to the presence of F (fMLFC). In HeLa FPR1-GFP cells treated with the D, E, F mixture, the red fluorescence did not colocalize with FPR1-GFP (Fig. 4B), indicating that DOX permeated into these cells without binding to FPR1. The Rr value of D, E, F mixture (0.015) also indicated that the

internalized D, E, F mixture were not colocalized with FPR1 (Fig. 4C). These results demonstrated that simply mixing D, E, F did not produce the same effect of DEF. It should be noted that the intensity of cell-associated red fluorescence after exposure to DEF is much weaker than that of DOX alone and of the D, E, F mixture (Fig. 4B). The possible reason for this phenomenon is that DOX enters into cells more freely through passive diffusion [42], whereas DEF internalization through FPR1 had a much smaller capacity. In addition, the low solubility of DEF in water also limited the uptake of DEF. Therefore, the entry of DOX and DEF were not comparable as they employ different mechanisms. Because DE mostly remained outside the HeLa and HeLa FPR1-GFP cells (Fig. 4A and 4B), it served as an excellent control for FPR1-dependent internalization. These results were summarized in a bar graph (Fig. 4D).

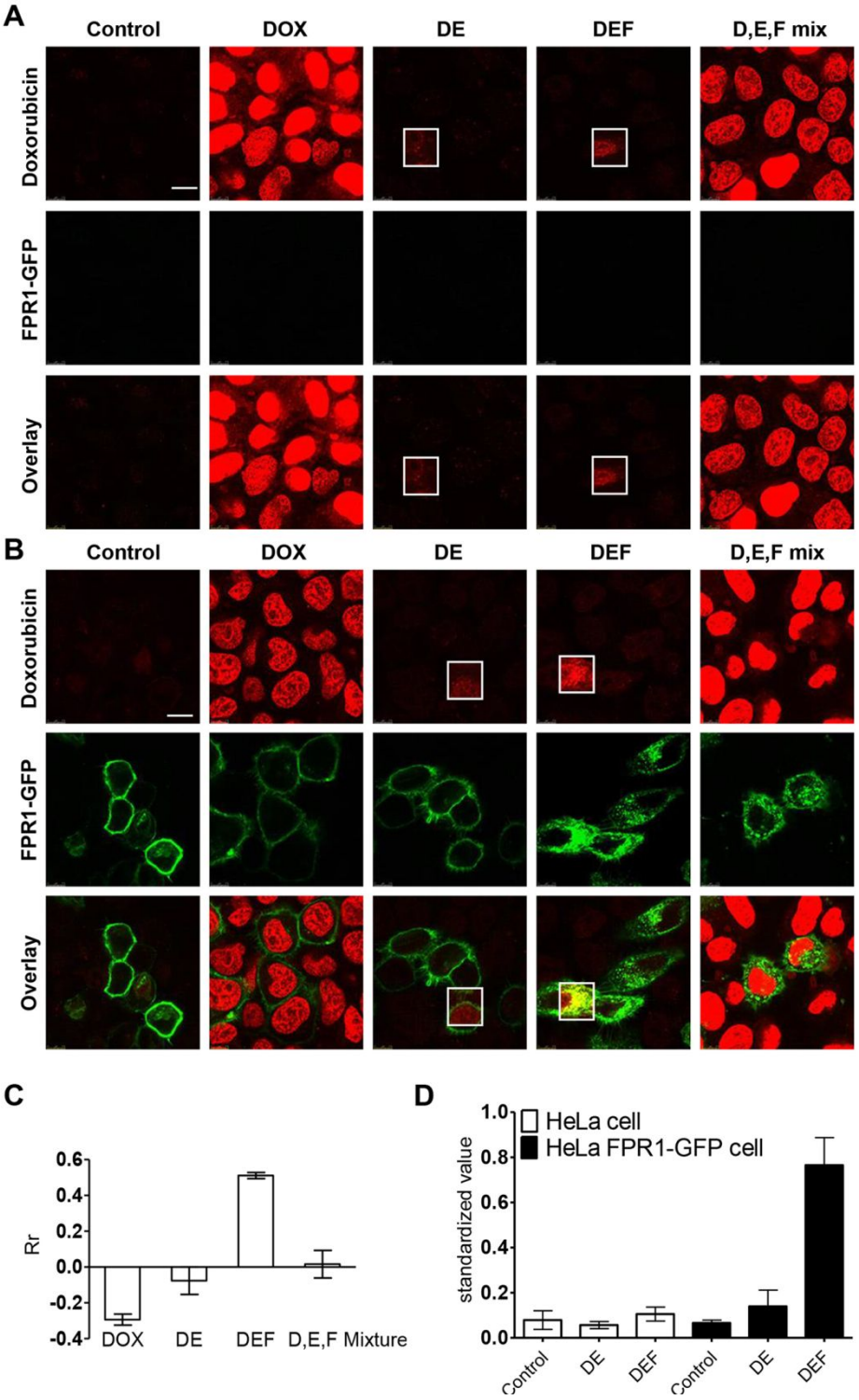

Fig. 4. Cellular uptake of DOX, DE, DEF and the mixture of D, E and F. Each component at the concentration of 5 μM was measured for cellular uptake in (A) HeLa cells and (B) HeLa FPR1-GFP cells. The exposure of the framed areas has been manually increased by 4-fold in order to more clearly view the fluorescence colocalization. DOX and its conjugate carried red fluorescence, whereas FPR1-GFP carried green fluorescence. For controls, culture medium without ligand was added to the cells. All samples were stimulated with compounds for 1 h at 37°C. Cellular uptake was determined by fluorescent confocal microscopy. Scale

bar = 10 μm. (C) Fluorescence colocalization analysis of DOX, DE, DEF and the D, E, F mixture. Pearson's correlation coefficient (Rr) for colocalization of red fluorescence with FPR1-GFP green fluorescence was obtained with the Image J plugin, Colocalization Finder. (D) Standardized fluorescence intensities of HeLa cells and HeLa FPR1-GFP cells were quantified using the Image J software. The data shown are mean ± SEM (n=3). *, $p<0.05$, **, $p<0.01$, ***, $p<0.001$.

3.4. Trafficking of DEF-FPR1 after internalization

3.4.1. FPR1 entry into endosomes after internalization

In most endocytosis pathways, vesicles are delivered to endosomes and lysosomes [17]. There are however exceptions such as in caveolae-mediated endocytosis, where internalized substances are transported to endoplasmic reticulum (ER) instead of endosomes and lysosomes [43-44]. To determine the route of internalized DEF, we used a fluorescent lysosome tracker (LysoTracker) and early endosome-RFP as markers for lysosomes and endosomes, respectively. DEF was applied to cells to induce internalization of FPR1-GFP or FPR1-mruby2, which led to internalization of FPR1 as evidenced by the intracellular appearance of green and red fluorescence (Fig. 5A). The level of FPR1 colocalization with endosome was higher than that of lysosome (yellow dot in the endosome group). The results demonstrated that the most of internalized FPR1-GFP were entered endosome.

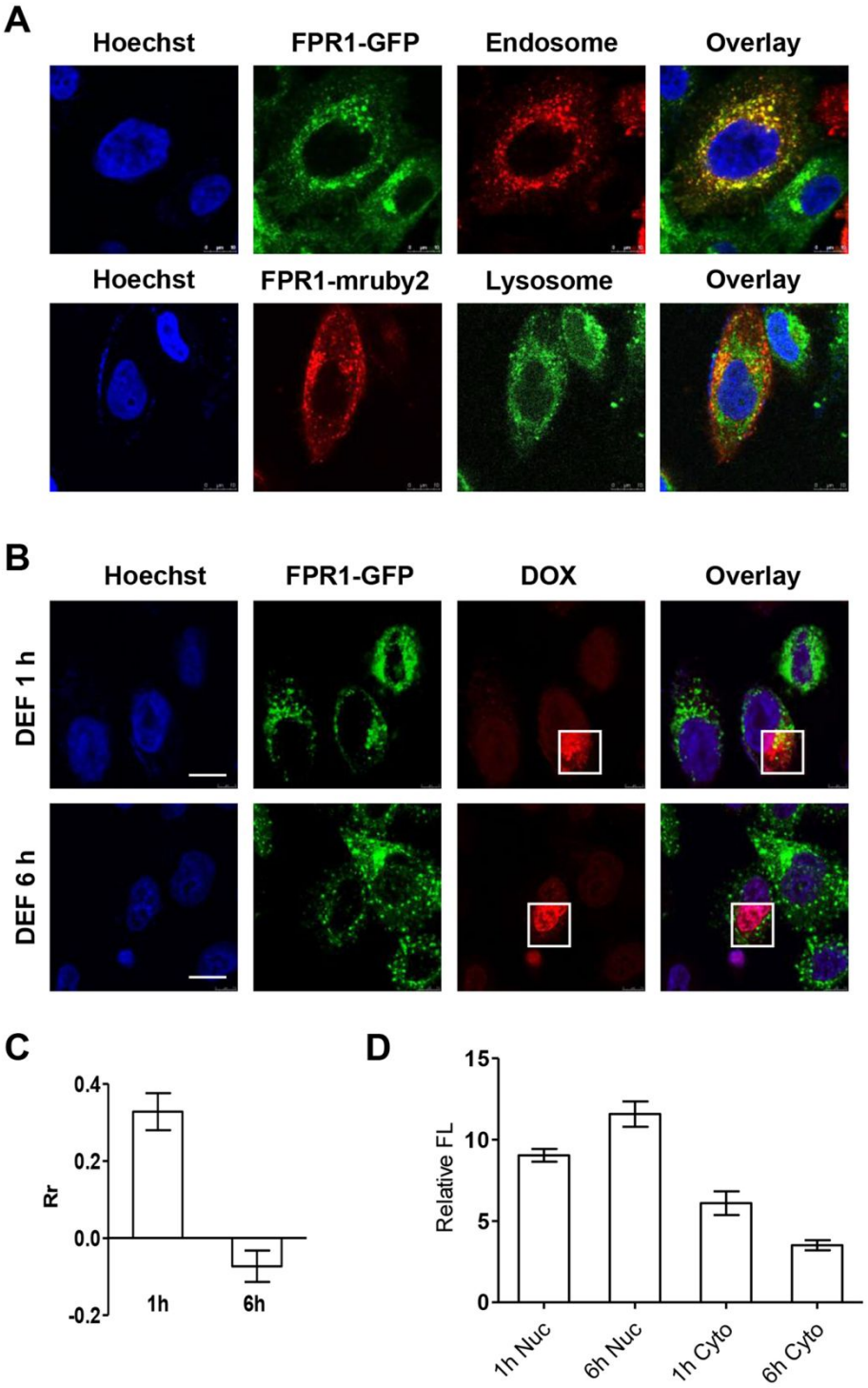

Fig. 5. Colocalization study of FPR1 with lysosome and endosome and intracellular pH-induced release of DOX from DEF. (A) Endosome-RFP was used for staining of endosome at 37°C for 16 h (upper panels). Lysotracker yellow HCK-123 (2 μM) was used to stain lysosome for 1 h at 37°C (lower panels). Then the cells were treated with 5 μM of DEF at 37°C for 1 h to induce FPR1 internalization. The nucleus (blue channel) was stained with 2 μg/mL Hoechst for 10 min at room temperature. Scale bar = 10 μm. (B) HeLa FPR1-GFP cells were treated with DEF for 1 h (upper panels) and 6 h (lower panels). The exposure in the framed areas was adjusted by a 4-fold increase to better visualize colocalization of the

two molecules. Blue, green and red colors represent the nucleus, FPR1-GFP and DOX, respectively. Scale bar = 10 μm. (C) Fluorescence colocalization analysis. Pearson's correlation coefficient (Rr) for colocalization of red fluorescence with green fluorescence (FPR1-GFP) was obtained with the Image J software plugin, Colocalization Finder. (D) Quantification of red fluorescence intensity in nucleus and cytoplasm after treatment with DEF for 1 h and 6 h. The data are means ± SEM (n=3). *, $p<0.05$, **, $p<0.01$ and ***, $p<0.001$.

3.4.2. pH-sensitive release of DOX and its entry into nucleus

In the present study, the pH-sensitive peptide conjugate (DEF) carries a hydrazone bond between DOX and the EMCH linker. This bond is stable at neutral pH but hydrolyzed at lower pH in an acidic cellular compartment such as endosome (pH 5.0-6.5) and lysosome (pH 4.5-5.0) [45-46]. Hydrazone is widely used in pH-sensitive drug delivery [47-49]. The release behavior was tested in the HeLa FPR1-GFP cells. As shown in Fig. 5B, FPR1-GFP was internalized into cells after binding of DEF. One hour after initiation of the internalization assay, the majority of the ligand (red fluorescence) was colocalized with FPR1 (green fluorescence) as evidenced in the overlay. The Rr value of 0.32 also support DEF colocalization with FPR1 at 1 h (Fig. 5C). A small amount of red fluorescence was detectable in the nucleus, consistent with the propensity of DOX to enter into nucleus. Six hours after initiation of internalization, the red fluorescence was visible only in the nucleus while the green fluorescence remained in the cytoplasm (Fig. 5B). Given that DEF is not cell membrane permeable and therefore cannot escape from the endosome, these results indicate that DOX was released from DEF in the endosome and then moved to the nucleus between 1 h and 6 h. An Rr value of -0.07 support separation of DOX from FPR1. Fig. 5D summarizes relative distribution of red fluorescence in the nucleus *vs.* cytoplasm 1 h and 6 h after agonist-induced FPR1 internalization.

3.5. Endocytosis mechanisms underlying DEF-induced FPR1 internalization

3.5.1. Effect of endocytosis inhibitors on FPR1 internalization

To study the endocytic pathways involved in the internalization of FPR1. HeLa FPR1-GFP cells were treated with different pharmacological inhibitors of clathrin-mediated endocytosis, caveolae-mediated endocytosis, macropinocytosis and phagocytosis (Fig. 6). Sucrose and MDC were used as inhibitors of clathrin-mediated endocytosis [19, 50]. Filipin complex as sterol-binding agent was used to inhibit the caveolae-mediated endocytosis [12, 51].

Cytochalasins were a group of fungal metabolites that could bind to actin filaments to block the polymerization of actin. Both cytochalasins D (Cyto D) and B (Cyto B) can disrupt actin polymerization [52-53] . Cyto D was often used as an inhibitor of macropinocytosis [15, 31]. Cyto B was used to inhibit phagocytosis [19, 54]. As shown in Fig. 6 (panels c to g), none of the pharmacological inhibitors prevented the internalization of FPR1 (green fluorescence in cytoplasm). The results suggest that FPR1 internalization induced by DEF was independent of clathrin, caveolin, macropinocytosis and phagocytosis. These findings are consistent with a previous report that fMLF-stimulated FPR1 is internalized through a clathrin-independent pathway [25].

It was reported that plasma membrane cholesterol plays an important role in different endocytosis pathways such as clathrin-mediated endocytosis, caveolae-mediated endocytosis and micropinocytosis. [55-58]. To deplete the plasma membrane cholesterol, HeLa FPR1-GFP cells were treated with MβCD and lovastatin. MβCD extracts cholesterol from the cell membrane and lovastatin inhibits the synthesis of cholesterol [15, 59]. Fig. 6h showed that the treatment prevented DEF-induced FPR1 internalization as the green fluorescence remained on cell surface membrane. Thus, depletion of plasma membrane cholesterol led to inhibition of FPR1 internalization, suggesting that cholesterol plays an important role in FPR1 internalization. Since lipid raft contains both cholesterol and sphingolipids, the result may also suggest an involvement of lipid raft in DEF-induced FPR1 internalization.

Microtubules are multifunctional cytoskeletal filaments formed through the polymerization of α-tubulin and β-tubulin, which plays an important role in intracellular transportation [60-61]. In the present study, nocodazole was used as a microtubule-disrupting agent for study of the function of microtubule in FPR1 internalization. As shown in Fig. 6i, FPR1 (green fluorescence) accumulated in the perinuclear region in nocodazole-treated samples, suggesting that FPR1 internalization was not prevented by disruption of microtubules.

The cytotoxicity of different pharmacological inhibitors was determined by MTT colorimetric test. All inhibitors did not affect cell viability at the concentration and incubation time used in our experiment (Supplemental Fig. 1).

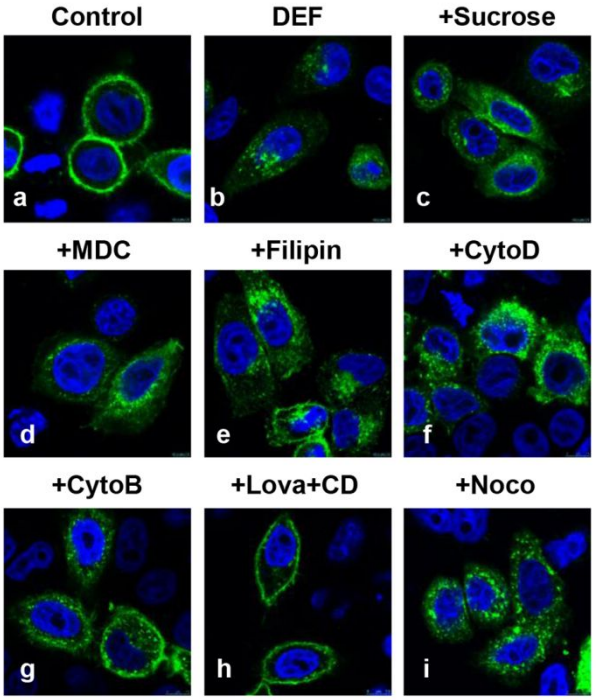

Fig. 6. Effects of different pharmacological inhibitors on the internalization of FPR1. The HeLa FPR1-GFP cells were pretreated with different inhibitors at 37°C for 30 min in DMEM containing 0.5M sucrose, 100 μM MDC, 5 μg/mL Filipin complex, 10 μM CytoD or for 2 h at 37°C in DMEM containing 10 μg/mL CytoB or for 2 h at 37°C in DMEM containing 10 μg/mL cytochalasin B (Cyto B), or for 1 h at 37°C in DMEM containing 3 μg/mL Lovastatin + 10 mM MβCD (Lova + CD), 10 μg/mL nocodazole (Noco). The cells were then treated with 5 μM DEF at 37°C for 1 h except the control group, which was not subject to agonist stimulation. Nuclei were stained with Hoechst (blue) and FPR1 was labeled with GFP (green). Scale bar = 20 μm.

3.5.2. Effect of different pharmacological inhibitors on the number of cell surface FPR1

To quantitatively study the mechanism for FPR1 internalization, an FPR1 antibody was used for detection of cell surface receptor using flow cytometry. As a complementary method to confocal microscopy, flow cytometry provides a quantitative measurement of the effect of different inhibitors on FPR1 internalization. As shown in Supplemental Fig. 2, most FPR1 proteins are present on the cell surface. After treating with DEF for 1 h, approximately 80% of the receptor was internalized into the cells (Supplemental Fig. 2, DEF group). There was no significant difference in cell surface receptor number between the DEF group and any one of the endocytosis inhibitor groups (sucrose, MDC, filipin complex, cyto B, cyto D). Therefore, none of the endocytosis pathway inhibitors could prevent DEF-induced FPR1

internalization. This result is consistent with the findings from the confocal and siRNA knockdown experiments. The microtubule disruption group (nocodazole treated) also did not show any significant difference from DEF alone, consistent with the microscopic results and together suggest that internalization of FPR1 is not affected by disruption of microtubules. However, there was a significant difference between the cholesterol depletion group (Lova + CD) and DEF group. The cell surface receptor number was nearly the same as in the control group, indicating minimal internalization of FPR1. The result is consistent with the microscopic data and demonstrate an important role for cholesterol in the process of FPR1 internalization.

3.5.3. Effect of siRNA on FPR1 internalization

siRNA can be designed to knockdown specific protein expression. It complements the use of pharmacological inhibitors. As an additional approach to our study of FPR1 internalization mechanism, siRNA targeting CHC (si-CHC) was used to knockdown the endocytic protein clathrin heavy chain (CHC) that regulates the clathrin-mediated endocytosis. In addition, siRNA targeting CAV1 (si-CAV1) was used to silence expression of caveolin-1 that plays an important role in caveolin-dependent endocytosis. PAK1 has an important impact on the closure of macropinocytic cup and the polymerization of actin. Macropinocytosis can be inhibited by siRNA knock down of PAK1 (si-PAK1). As Fig. 7A shows, the FPR1 lies on the cell surface in control siRNA-transfected HeLa FPR1-GFP cells (si-cont group). FPR1 was internalized into cells following DEF stimulation (si-cont+DEF group). For siRNA treated group (si-CHC, si-CAV1 and si-PAK1), siRNA transfection failed to inhibit the internalization of FPR1, which indicated that FPR1 was not internalized through clathrin-mediated or caveolin-mediated endocytosis and macropinocytosis.

To estimate the gene silence efficiency induced by the siRNA, HeLa FPR1-GFP cells were transfected with negative siRNA (served as a control) and siRNA targeting to CHC, CAV1 and PAK1. The mRNA levels of the targeted cells were examined by Q-PCR. The mRNA levels of CHC, CAV1 and PAK1 were decreased after transfection with siRNA compared with the control group (Fig. 7B). The results demonstrated that siRNA transfection could effectively suppress the expression of the mRNA of interest. There is also a positive correlation between the mRNA expression level and the protein expression level. Therefore,

we can conclude that the siRNA knockdown approach used in this study successfully silenced the expression of the proteins of interest.

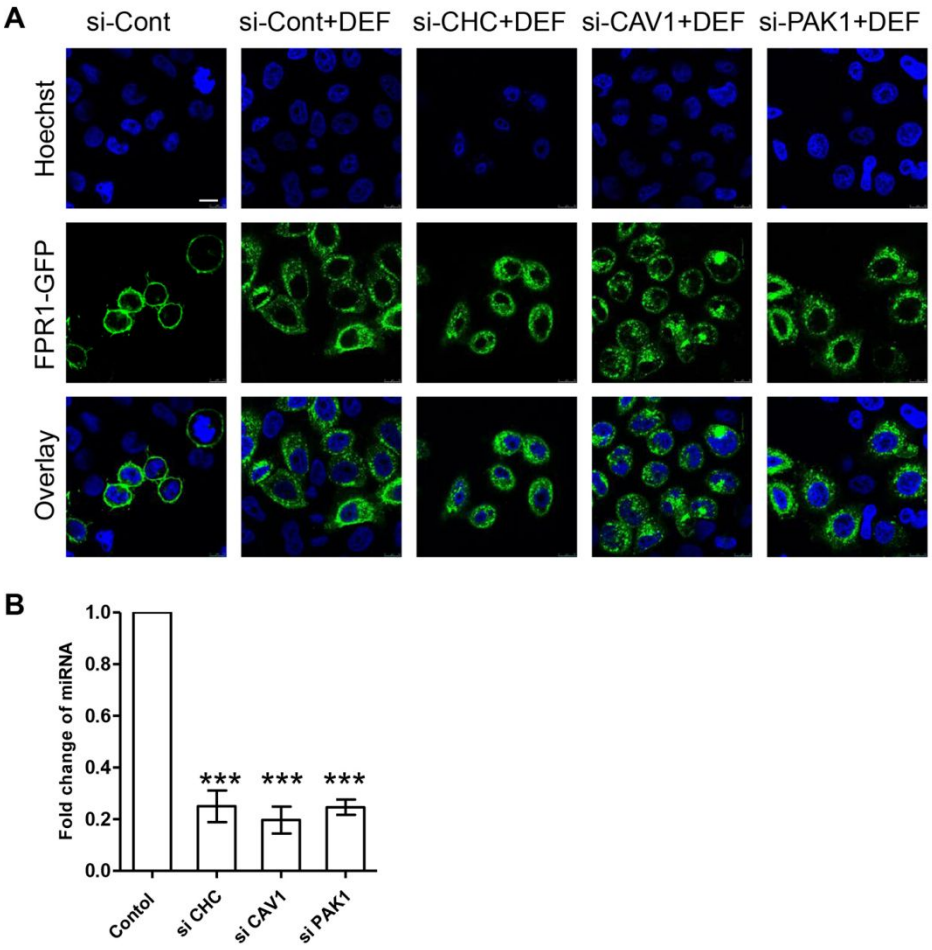

Fig. 7. Effects of siRNA knock down of endocytosis-related proteins on FPR1 internalization. (A) Confocal images of siRNA transfected HeLa FPR1-GFP cells are shown. The cells were transfected with negative control siRNA (si-cont) or siRNA targeting CHC (si-CHC), CAV1 (si-CAV1) and PAK1 (si-PAK1) for 48 h and then treated with 5 μM DEF for 1 h at 37°C. Blue fluorescence is nucleus and green fluorescence is FPR1-GFP. Scale bar = 20 μm. (B) Expression of CHC, CAV1 and PAK1 mRNA after siRNA Knockdown experiments was determined by Q-PCR. The cell transfected with si-CHC, si-CAV1 and si-PAK1 along with negative siRNA served as controls to estimate the knockdown efficiency of each siRNA. Y axis represents the fold change of different mRNA (CHC, CAV1 and PAK1) compared with control group. The data shown are means ± SEM (n=3). *, $p<0.05$, **, $p<0.01$,***, $p<0.001$.

4. Discussion

The present study provides a prototype of cell surface receptor-mediated delivery of a drug complex, in which the drug in its freeform is otherwise lipid membrane permeable.

DOX, like many other anti-cancer drugs, enters freely into cells and functions in the nucleus. DOX is an anthracycline that exerts its anti-cancer effect through inhibition of topoisomerase II [62]. Since topoisomerase II is also present in normal cells and plays a critical role in promoting chromosome disentanglement, DOX and similar agents can cause side effects in clinical use. It is therefore beneficial to deliver DOX only to selected types of cells. In the present study the drug conjugate DEF changes the lipid membrane permeating property of DOX through its conjugation to a peptide that cannot pass through the plasma membrane. As shown in our experimental data, the entry of DEF is dependent on the cell surface receptor, FPR1, confirming that DOX in the DEF conjugate is no longer able to enter cells through membrane diffusion.

FPR1 is one of the first identified chemoattractant receptors expressed primarily in phagocytes such as neutrophils [20]. Promyelocytic leukemic cells such as human HL-60 also express FPR1 [63], making it one of the potential targets for drug delivery into leukemic cells. The receptor belongs to the GPCR superfamily and is a rhodopsin-like (class A) receptor, and is known for its ability to bind peptides bearing a formylated methionione in the *N*-terminus, such as peptides derived from bacteria and mitochondria. The ligand binding pocket of FPR1 is sufficiently large to accommodate at least 5 amino acids based on a study using fluorescent formyl peptides [27]. Moreover, the *N*-terminus of the fluorescent peptide appears to insert deep into the binding pocket, making the C-terminus of the peptide available for coupling of relatively bulky molecules without compromising its binding to the receptor. This is confirmed in the present study, in which the DEF conjugate retained its receptor-binding property as well as biological activities. Like other GPCRs, FPR1 undergoes internalization upon ligand binding [24], effectively bringing the ligands into cells. The internalization of FPR1 shares many properties with other GPCRs such as the requirement for the NPXXY sequence motif in the 7th transmembrane domain [64]. Although the clarthrin-dependent internalization mechanism is common to most cell surface receptors including many GPCRs [65-66], ligand-induced internalization of FPR1 does not seem to use this classic pathway of receptor internalization [25]. Clathrin-independent endocytosis of receptors have seen increased reports in recent years [67]. In the present study, pharmacological inhibitors were used along with siRNA knockdown of protein expression to

study the pathways for FPR1 internalization. The change of cell surface receptor number was studied by using both qualitative analysis (confocal microscopy) and quantitative analysis (flow cytometry). The results obtained from these experiments show that internalization of FPR1 does not involve conventional endocytosis pathways including the clathrin-mediated and caveolin-mediated endocytosis, macropinocytosis and phagocytosis. Instead, membrane cholesterol plays an important role in FPR1 internalization, which is inhibited by the combined use of lovastatin and MβCD. We conclude that internalization of FPR1 is a cholesterol-dependent process.

Regardless of the endocytosis mechanism used in the internalization of FPR1, the DEF complex has been shown to enter the endosomes and then lysosomes, based on its colocalization with endosomal and lysosomal markers. This property has been used for the design of an acid-sensitive drug delivery approach through incorporation of the EMCH bond that can be cleaved in an acidic environment [41]. In the low-pH intracellular compartments, the DEF dissociates from the receptor as previously documented [24-25, 68]. It is expected that DOX separates from the acid-sensitive EMCH linker with its cleavage [41]. Once DOX regain its membrane permeable property, it moves to the nucleus and binds to its target, topoisomerase II. We have shown nuclear localization of DOX only after incubating FPR1-expressing cells with DEF, and in the time sequence that support receptor-mediated delivery of the DEF complex to intracellular compartments. This approach may be adapted for delivery of other drugs through cell surface receptors such as GPCRs. It is still unclear whether DEF is stable in vivo, but studies conducted previously using similar DE-conjugated proteins found that the drug-protein complex to be stable in the plasma [41, 69], suggesting feasibility of using this approach for targeted drug delivery.

Since FPR1 is expressed in phagocytes, such as macrophages that serves as a long-term reservoir of HIV-1, FPR1 may be a target for delivery of anti-HIV-1 drugs. There have been efforts in designing FPR1 ligand-based delivery approaches to macrophages [70-72]. These studies use PEG nanocarrier bearing multiple copies of fMLF for improved binding to macrophages through FPR1. For example, attachment of two copies of fMLF was shown to improve uptake of nanocarriers having the size of 40 nM. These studies, however, did not show whether the nanoparticles were taken up through FPR1 internalization, or through

other forms of internalization. As the studies shows, each ethylene glycol subunit in the PEG is tightly associated with two or three water molecules. Therefore, the nanocarriers are different from drug conjugates. The DEF conjugate used in the present study has the advantage of more precise delivery through a known receptor and its internalization route. One disadvantage is that each conjugate contains one drug molecule in the present design, which may be further improved in future studies.

5. Conclusions

In the present study, the acid-sensitive DOX conjugate (DEF) containing a formyl peptide was synthesized for FPR1-targeted drug delivery. Cellular uptake experiments and colocalization analysis demonstrate that DEF is excluded from cell membrane boundary but can enter into cells through FPR1 internalization. Once inside the acidic endosomes, DOX is released and then transported to the nucleus.

In conclusion, the present study demonstrates the feasibility of targeting FPR1 for drug delivery through the use the DEF conjugate. This approach may be used for FPR1-dependent uptake of drugs that are made impermeable to plasma membrane, such as DOX. Likewise, receptor internalization may be explored for delivery of drugs that are not permeable through plasma membrane, such as most peptides and other charged molecules. FPR1 is found at high abundance in myeloid cells such as macrophages, which serve as a reservoir for HIV-1. The ability of these cells to infiltrate in inflammatory tissues and organs make it feasible to carry drugs to these sites through blood circulation, taking full advantage of drug administration through transfusion. Future studies will explore the mechanism of FPR1 internalization for rational design of FPR1-based delivery of drugs.

Acknowledgements

The authors would like to thank members of the Ye Laboratory for helpful discussions. This work was supported in part by grants from the Science and Technology Development Fund of Macau (FDCT 026/2016/A1), from University of Macau (MYRG2016-00246-ICMS-QRCM).

Supporting Information

Cytotoxicity and cell surface receptor detection after treatment with pharmacological inhibitors.

References

1. Alberts, B.; Bray, D.; Hopkin, K.; Johnson, A.; Lewis, J.; Raff, M.; Roberts, K.; Walter, P., *Essential Cell Biology*. W. W. Norton & Company: 2013.

2. Kaksonen, M.; Roux, A., Mechanisms of clathrin-mediated endocytosis. *Nat Rev Mol Cell Biol* **2018,** *19* (5), 313-326.

3. Ho, Y. T.; Kamm, R. D.; Kah, J. C. Y., Influence of protein corona and caveolae-mediated endocytosis on nanoparticle uptake and transcytosis. *Nanoscale* **2018,** *10* (26), 12386-12397.

4. Peddi, S.; Pan, X.; MacKay, J. A., Intracellular Delivery of Rapamycin From FKBP Elastin-Like Polypeptides Is Consistent With Macropinocytosis. *Frontiers in pharmacology* **2018,** *9*, 1184.

5. Lancaster, C. E.; Ho, C. Y.; Hipolito, V. E. B.; Botelho, R. J.; Terebiznik, M. R., Phagocytosis: what's on the menu? *Biochem Cell Biol* **2018**, 1-9.

6. Navaroli, D. M.; Bellve, K. D.; Standley, C.; Lifshitz, L. M.; Cardia, J.; Lambright, D.; Leonard, D.; Fogarty, K. E.; Corvera, S., Rabenosyn-5 defines the fate of the transferrin receptor following clathrin-mediated endocytosis. *Proceedings of the National Academy of Sciences of the United States of America* **2012,** *109* (8), E471-80.

7. Mulkearns, E. E.; Cooper, J. A., FCH domain only-2 organizes clathrin-coated structures and interacts with Disabled-2 for low-density lipoprotein receptor endocytosis. *Mol Biol Cell* **2012,** *23* (7), 1330-42.

8. Fagerholm, S.; Ortegren, U.; Karlsson, M.; Ruishalme, I.; Stralfors, P., Rapid insulin-dependent

endocytosis of the insulin receptor by caveolae in primary adipocytes. *PLoS One* **2009,** *4* (6), e5985.

9. Ramzy, L.; Nasr, M.; Metwally, A. A.; Awad, G. A. S., Cancer nanotheranostics: A review of the role of conjugated ligands for overexpressed receptors. *Eur J Pharm Sci* **2017,** *104*, 273-292.

10. Guo, S.; Zhang, X.; Zheng, M.; Zhang, X.; Min, C.; Wang, Z.; Cheon, S. H.; Oak, M. H.; Nah, S. Y.; Kim, K. M., Selectivity of commonly used inhibitors of clathrin-mediated and caveolae-dependent endocytosis of G protein-coupled receptors. *Biochimica et biophysica acta* **2015,** *1848* (10 Pt A), 2101-10.

11. Kiss, A. L.; Botos, E., Endocytosis via caveolae: alternative pathway with distinct cellular compartments to avoid lysosomal degradation? *J Cell Mol Med* **2009,** *13* (7), 1228-37.

12. Kasai, H.; Inoue, K.; Imamura, K.; Yuvienco, C.; Montclare, J. K.; Yamano, S., Efficient siRNA delivery and gene silencing using a lipopolypeptide hybrid vector mediated by a caveolae-mediated and temperature-dependent endocytic pathway. *Journal of nanobiotechnology* **2019,** *17* (1), 11.

13. Lim, J. P.; Gleeson, P. A., Macropinocytosis: an endocytic pathway for internalising large gulps. *Immunol Cell Biol* **2011,** *89* (8), 836-43.

14. Costa Verdera, H.; Gitz-Francois, J. J.; Schiffelers, R. M.; Vader, P., Cellular uptake of extracellular vesicles is mediated by clathrin-independent endocytosis and macropinocytosis. *Journal of controlled release : official journal of the Controlled Release Society* **2017,** *266*, 100-108.

15. Rejman, J.; Oberle, V.; Zuhorn, I. S.; Hoekstra, D., Size-dependent internalization of particles via the pathways of clathrin-and caveolae-mediated endocytosis. *Biochemical Journal* **2004,** *377* (1), 159-169.

16. Arandjelovic, S.; Ravichandran, K. S., Phagocytosis of apoptotic cells in homeostasis. *Nat Immunol* **2015,** *16* (9), 907-17.

17. Canton, I.; Battaglia, G., Endocytosis at the nanoscale. *Chemical Society Reviews* **2012,** *41* (7), 2718-2739.

18. Flannagan, R. S.; Jaumouille, V.; Grinstein, S., The cell biology of phagocytosis. *Annu Rev Pathol* **2012,** *7*, 61-98.

19. Lunov, O.; Syrovets, T.; Loos, C.; Beil, J.; Delacher, M.; Tron, K.; Nienhaus, G. U.; Musyanovych, A.; Mailander, V.; Landfester, K.; Simmet, T., Differential uptake of functionalized polystyrene nanoparticles by human macrophages and a monocytic cell line. *ACS Nano* **2011,** *5* (3), 1657-69.

20. Ye, R. D.; Boulay, F.; Wang, J. M.; Dahlgren, C.; Gerard, C.; Parmentier, M.; Serhan, C. N.; Murphy, P. M., International Union of Basic and Clinical Pharmacology. LXXIII. Nomenclature for the formyl peptide receptor (FPR) family. *Pharmacol Rev* **2009,** *61* (2), 119-61.

21. Dahlgren, C.; Gabl, M.; Holdfeldt, A.; Winther, M.; Forsman, H., Basic characteristics of the neutrophil receptors that recognize formylated peptides, a danger-associated molecular pattern generated by bacteria and mitochondria. *Biochem Pharmacol* **2016,** *114*, 22-39.

22. He, H. Q.; Troksa, E. L.; Caltabiano, G.; Pardo, L.; Ye, R. D., Structural determinants for the interaction of formyl peptide receptor 2 with peptide ligands. *J Biol Chem* **2014,** *289* (4), 2295-306.

23. Migeotte, I.; Riboldi, E.; Franssen, J. D.; Gregoire, F.; Loison, C.; Wittamer, V.; Detheux, M.; Robberecht, P.; Costagliola, S.; Vassart, G.; Sozzani, S.; Parmentier, M.; Communi, D., Identification and characterization of an endogenous chemotactic ligand specific for FPRL2. *J Exp Med* **2005,** *201* (1), 83-93.

24. Niedel, J. E.; Kahane, I.; Cuatrecasas, P., Receptor-mediated internalization of fluorescent chemotactic peptide by human neutrophils. *Science* **1979,** *205* (4413), 1412-4.

25. Gilbert, T. L.; Bennett, T. A.; Maestas, D. C.; Cimino, D. F.; Prossnitz, E. R., Internalization of the

human N-formyl peptide and C5a chemoattractant receptors occurs via clathrin-independent mechanisms. *Biochemistry* **2001,** *40* (12), 3467-75.

26. He, H. Q.; Ye, R. D., The Formyl Peptide Receptors: Diversity of Ligands and Mechanism for Recognition. *Molecules* **2017,** *22* (3), 455.

27. Sklar, L. A.; Fay, S. P.; Seligmann, B. E.; Freer, R. J.; Muthukumaraswamy, N.; Mueller, H., Fluorescence Analysis of the Size of a Binding Pocket of a Peptide Receptor at Natural Abundance. *Biochemistry* **1990,** *29* (2), 313-316.

28. Nanamori, M.; Cheng, X.; Mei, J.; Sang, H.; Xuan, Y.; Zhou, C.; Wang, M. W.; Ye, R. D., A novel nonpeptide ligand for formyl peptide receptor-like 1. *Mol Pharmacol* **2004,** *66* (5), 1213-22.

29. Willner, D.; Trail, P. A.; Hofstead, S. J.; King, H. D.; Lasch, S. J.; Braslawsky, G. R.; Greenfield, R. S.; Kaneko, T.; Firestone, R. A., (6-Maleimidocaproyl)hydrazone of doxorubicin--a new derivative for the preparation of immunoconjugates of doxorubicin. *Bioconjug Chem* **1993,** *4* (6), 521-7.

30. Adler, J.; Parmryd, I., Quantifying Colocalization by Correlation: The Pearson Correlation Coefficient is Superior to the Mander's Overlap Coefficient. *Cytometry Part A* **2010,** *77a* (8), 733-742.

31. Al Soraj, M.; He, L.; Peynshaert, K.; Cousaert, J.; Vercauteren, D.; Braeckmans, K.; De Smedt, S.; Jones, A. T., siRNA and pharmacological inhibition of endocytic pathways to characterize the differential role of macropinocytosis and the actin cytoskeleton on cellular uptake of dextran and cationic cell penetrating peptides octaarginine (R8) and HIV-Tat. *Journal of controlled release* **2012,** *161* (1), 132-141.

32. Motley, A.; Bright, N. A.; Seaman, M. N. J.; Robinson, M. S., Clathrin-mediated endocytosis in AP-2-depleted cells. *J. Cell Biol.* **2003,** *162* (5), 909-918.

33. Livak, K. J.; Schmittgen, T. D., Analysis of relative gene expression data using real-time

quantitative PCR and the 2(-Delta Delta C(T)) Method. *Methods* **2001,** *25* (4), 402-8.

34. Chan, C. Y.; Pedley, A. M.; Kim, D.; Xia, C.; Zhuang, X.; Benkovic, S. J., Microtubule-directed transport of purine metabolons drives their cytosolic transit to mitochondria. *Proceedings of the National Academy of Sciences of the United States of America* **2018,** *115* (51), 13009-13014.

35. He, H. Q.; Liao, D.; Wang, Z. G.; Wang, Z. L.; Zhou, H. C.; Wang, M. W.; Ye, R. D., Functional characterization of three mouse formyl peptide receptors. *Mol Pharmacol* **2013,** *83* (2), 389-98.

36. Sheng, Y.; Xu, J.; You, Y.; Xu, F.; Chen, Y., Acid-Sensitive Peptide-Conjugated Doxorubicin Mediates the Lysosomal Pathway of Apoptosis and Reverses Drug Resistance in Breast Cancer. *Mol Pharm* **2015,** *12* (7), 2217-28.

37. Walker, L.; Perkins, E.; Kratz, F.; Raucher, D., Cell penetrating peptides fused to a thermally targeted biopolymer drug carrier improve the delivery and antitumor efficacy of an acid-sensitive doxorubicin derivative. *Int J Pharm* **2012,** *436* (1-2), 825-32.

38. Moktan, S.; Perkins, E.; Kratz, F.; Raucher, D., Thermal targeting of an acid-sensitive doxorubicin conjugate of elastin-like polypeptide enhances the therapeutic efficacy compared with the parent compound in vivo. *Mol Cancer Ther* **2012,** *11* (7), 1547-56.

39. Markovsky, E.; Baabur-Cohen, H.; Satchi-Fainaro, R., Anticancer polymeric nanomedicine bearing synergistic drug combination is superior to a mixture of individually-conjugated drugs. *Journal of Controlled Release* **2014,** *187*, 145-157.

40. Scomparin, A.; Salmaso, S.; Bersani, S.; Satchi-Fainaro, R.; Caliceti, P., Novel folated and non-folated pullulan bioconjugates for anticancer drug delivery. *Eur J Pharm Sci* **2011,** *42* (5), 547-58.

41. Kratz, F.; Warnecke, A.; Scheuermann, K.; Stockmar, C.; Schwab, J.; Lazar, P.; Druckes, P.; Esser, N.; Drevs, J.; Rognan, D.; Bissantz, C.; Hinderling, C.; Folkers, G.; Fichtner, I.; Unger, C., Probing the

cysteine-34 position of endogenous serum albumin with thiol-binding doxorubicin derivatives. Improved efficacy of an acid-sensitive doxorubicin derivative with specific albumin-binding properties compared to that of the parent compound. *Journal of Medicinal Chemistry* **2002,** *45* (25), 5523-5533.

42. Chen, V. Y.; Posada, M. M.; Zhao, L.; Rosania, G. R., Rapid doxorubicin efflux from the nucleus of drug-resistant cancer cells following extracellular drug clearance. *Pharm Res* **2007,** *24* (11), 2156-67.

43. Shin, J. S.; Abraham, S. N., Caveolae as portals of entry for microbes. *Microbes and Infection* **2001,** *3* (9), 755-761.

44. Pelkmans, L.; Kartenbeck, J.; Helenius, A., Caveolar endocytosis of simian virus 40 reveals a new two-step vesicular-transport pathway to the ER. *Nat Cell Biol* **2001,** *3* (5), 473-83.

45. Chang, M. L.; Zhang, F.; Wei, T.; Zuo, T. T.; Guan, Y. Y.; Lin, G. M.; Shao, W., Smart linkers in polymer-drug conjugates for tumor-targeted delivery. *Journal of Drug Targeting* **2016,** *24* (6), 475-491.

46. Kanamala, M.; Wilson, W. R.; Yang, M.; Palmer, B. D.; Wu, Z., Mechanisms and biomaterials in pH-responsive tumour targeted drug delivery: A review. *Biomaterials* **2016,** *85*, 152-67.

47. Wang, J.; Bhattacharyya, J.; Mastria, E.; Chilkoti, A., A quantitative study of the intracellular fate of pH-responsive doxorubicin-polypeptide nanoparticles. *Journal of controlled release : official journal of the Controlled Release Society* **2017,** *260*, 100-110.

48. Sonawane, S. J.; Kalhapure, R. S.; Govender, T., Hydrazone linkages in pH responsive drug delivery systems. *Eur J Pharm Sci* **2017,** *99*, 45-65.

49. Hou, G.; Qian, J.; Xu, W.; Sun, T.; Wang, Y.; Wang, J.; Ji, L.; Suo, A., A novel pH-sensitive targeting polysaccharide-gold nanorod conjugate for combined photothermal-chemotherapy of breast cancer. *Carbohydrate polymers* **2019,** *212*, 334-344.

50. Zhou, J. X.; Liao, D.; Zhang, S.; Cheng, N.; He, H. Q.; Ye, R. D., Chemerin C9 peptide induces receptor internalization through a clathrin-independent pathway. *Acta Pharmacologica Sinica* **2014,** *35* (5), 653-663.

51. Shuvaev, V. V.; Kiseleva, R. Y.; Arguiri, E.; Villa, C. H.; Muro, S.; Christofidou-Solomidou, M.; Stan, R. V.; Muzykantov, V. R., Targeting superoxide dismutase to endothelial caveolae profoundly alleviates inflammation caused by endotoxin. *Journal of controlled release : official journal of the Controlled Release Society* **2018,** *272*, 1-8.

52. Chia, J. X.; Efimova, N.; Svitkina, T. M., Neurite outgrowth is driven by actin polymerization even in the presence of actin polymerization inhibitors. *Mol Biol Cell* **2016**.

53. Kim, M. Y.; Kim, J. H.; Cho, J. Y., Cytochalasin B modulates macrophage-mediated inflammatory responses. *Biomolecules & therapeutics* **2014,** *22* (4), 295-300.

54. Yan, Z.; Wang, W.; Wu, Y.; Wang, W.; Li, B.; Liang, N.; Wu, W., Zinc oxide nanoparticle-induced atherosclerotic alterations in vitro and in vivo. *International journal of nanomedicine* **2017,** *12*, 4433-4442.

55. Rodal, S. K.; Skretting, G.; Garred, O.; Vilhardt, F.; van Deurs, B.; Sandvig, K., Extraction of cholesterol with methyl-beta-cyclodextrin perturbs formation of clathrin-coated endocytic vesicles. *Mol Biol Cell* **1999,** *10* (4), 961-74.

56. Subtil, A.; Gaidarov, I.; Kobylarz, K.; Lampson, M. A.; Keen, J. H.; McGraw, T. E., Acute cholesterol depletion inhibits clathrin-coated pit budding. *Proceedings of the National Academy of Sciences of the United States of America* **1999,** *96* (12), 6775-80.

57. Breen, M. R.; Camps, M.; Carvalho-Simoes, F.; Zorzano, A.; Pilch, P. F., Cholesterol depletion in adipocytes causes caveolae collapse concomitant with proteosomal degradation of cavin-2 in a switch-

like fashion. *PLoS One* **2012,** *7* (4), e34516.

58. Grimmer, S.; van Deurs, B.; Sandvig, K., Membrane ruffling and macropinocytosis in A431 cells require cholesterol. *J Cell Sci* **2002,** *115* (Pt 14), 2953-62.

59. Sarkar, P.; Chakraborty, H.; Chattopadhyay, A., Differential Membrane Dipolar Orientation Induced by Acute and Chronic Cholesterol Depletion. *Scientific reports* **2017,** *7* (1), 4484.

60. Akhmanova, A.; Steinmetz, M. O., Control of microtubule organization and dynamics: two ends in the limelight. *Nat Rev Mol Cell Biol* **2015,** *16* (12), 711-26.

61. Banerjee, S.; Hwang, D. J.; Li, W.; Miller, D. D., Current Advances of Tubulin Inhibitors in Nanoparticle Drug Delivery and Vascular Disruption/Angiogenesis. *Molecules* **2016,** *21* (11), 1468.

62. Nitiss, J. L., Targeting DNA topoisomerase II in cancer chemotherapy. *Nat Rev Cancer* **2009,** *9* (5), 338-50.

63. Rincon, E.; Rocha-Gregg, B. L.; Collins, S. R., A map of gene expression in neutrophil-like cell lines. *BMC genomics* **2018,** *19* (1), 573.

64. He, R.; Browning, D. D.; Ye, R. D., Differential roles of the NPXXY motif in formyl peptide receptor signaling. *J Immunol* **2001,** *166* (6), 4099-105.

65. Mettlen, M.; Chen, P. H.; Srinivasan, S.; Danuser, G.; Schmid, S. L., Regulation of Clathrin-Mediated Endocytosis. *Annu Rev Biochem* **2018,** *87*, 871-896.

66. Tsao, P.; Cao, T.; von Zastrow, M., Role of endocytosis in mediating downregulation of G-protein-coupled receptors. *Trends Pharmacol Sci* **2001,** *22* (2), 91-6.

67. Sandvig, K.; Kavaliauskiene, S.; Skotland, T., Clathrin-independent endocytosis: an increasing degree of complexity. *Histochem Cell Biol* **2018,** *150* (2), 107-118.

68. Rabiet, M. J.; Huet, E.; Boulay, F., The N-formyl peptide receptors and the anaphylatoxin C5a

receptors: an overview. *Biochimie* **2007,** *89* (9), 1089-106.

69. Kratz, F., INNO-206 (DOXO-EMCH), an albumin-binding prodrug of doxorubicin under development for phase II studies. *Current Bioactive Compounds* **2011,** *7* (1), 33-38.

70. Pooyan, S.; Qiu, B.; Chan, M. M.; Fong, D.; Sinko, P. J.; Leibowitz, M. J.; Stein, S., Conjugates bearing multiple formyl-methionyl peptides display enhanced binding to but not activation of phagocytic cells. *Bioconjug Chem* **2002,** *13* (2), 216-23.

71. Wan, L.; Pooyan, S.; Hu, P.; Leibowitz, M. J.; Stein, S.; Sinko, P. J., Peritoneal macrophage uptake, pharmacokinetics and biodistribution of macrophage-targeted PEG-fMLF (N-formyl-methionyl-leucyl-phenylalanine) nanocarriers for improving HIV drug delivery. *Pharm Res* **2007,** *24* (11), 2110-2119.

72. Wan, L.; Zhang, X.; Pooyan, S.; Palombo, M. S.; Leibowitz, M. J.; Stein, S.; Sinko, P. J., Optimizing size and copy number for PEG-fMLF (N-formyl-methionyl-leucyl-phenylalanine) nanocarrier uptake by macrophages. *Bioconjugate chemistry* **2007,** *19* (1), 28-38.

For Table of Contents Use Only

Targeted delivery of a ligand-drug conjugate via formyl peptide receptor 1 through cholesterol-dependent endocytosis

Junlin Wang, Meiwan Chen, Shaoping Li, Richard D. Ye

Graphical abstract

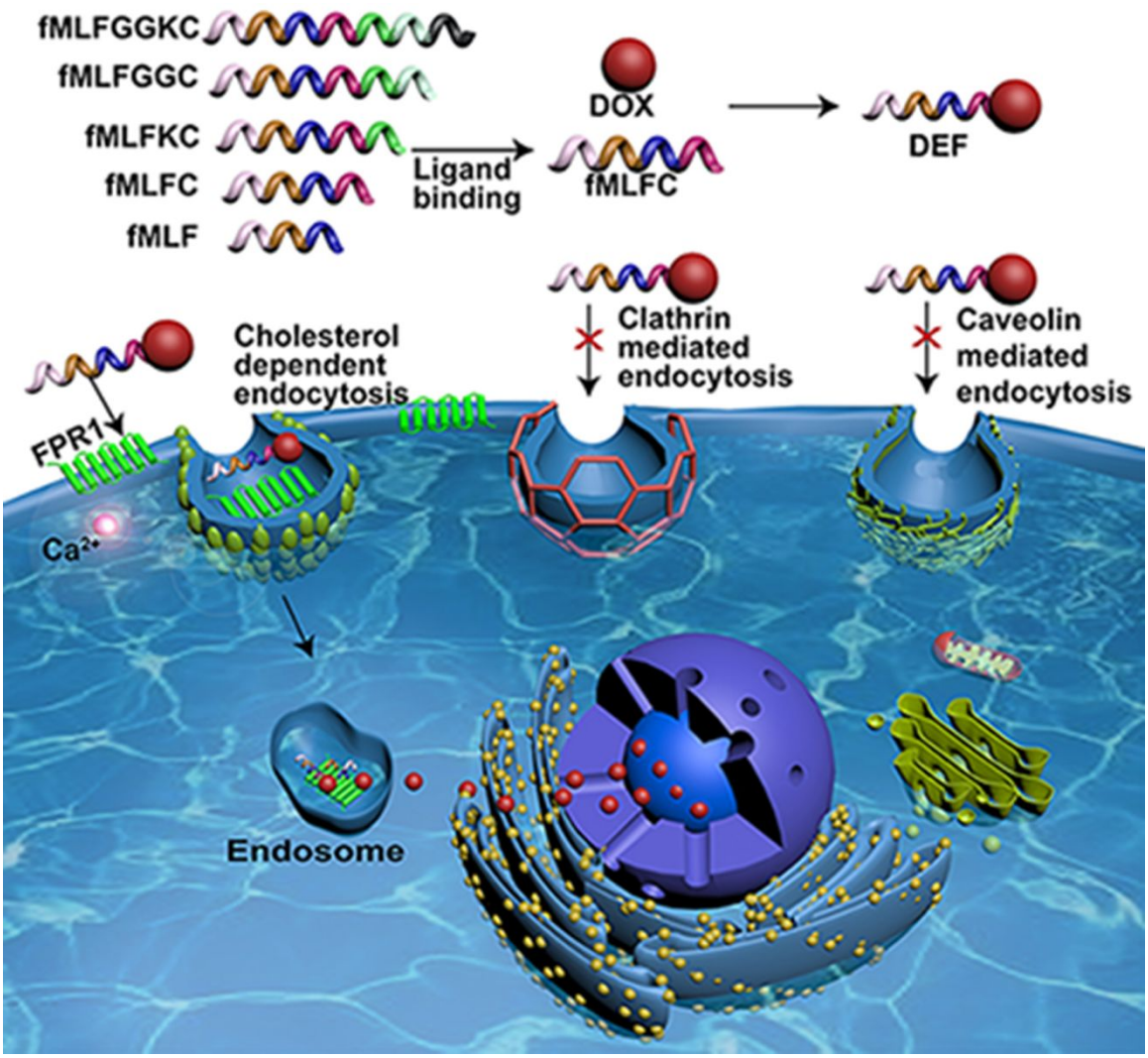
fMLFGGKC
fMLFGGC
fMLFKC
fMLFC
fMLF
Ligand binding
DOX
fMLFC
DEF
Cholesterol dependent endocytosis
Clathrin mediated endocytosis
Caveolin mediated endocytosis
FPR1
Ca2+
Endosome

1

2